Supporting Information

Unraveling Fluctuation in Gelatin and Monovalent Salt System: Coulombic Starvation

*Tithi Basu[a], Sunetra V. Chituru[a] and Saptarshi Majumdar[a]**

[a]Department of Chemical Engineering, Indian Institute of Technology Hyderabad, Sangareddy, Telangana 502284, India

*E-mail: saptarshi@che.iith.ac.in

S1. Materials and Methods

Gelatin, (Type-A, gel strength-175 and 300 Bloom, isoelectric pH 7-9) were purchased from Sigma Aldrich, and Sodium Chloride (NaCl) crystalline powder (PDV 99+%) was purchased from Alfa Aesar. Sodium Hydroxide (NaOH) pellets and Hydrochloride acid (HCl) (35%) were purchased from Qualigens and used for adjusting pH. Sodium alginate (SA; high viscosity, 1000–1500 cps, 1% in water), potassium chloride (KCl, ACS 99%), sodium hydrogen phosphate (Na_2HPO_4, ACS 99%), and potassium dihydrogen phosphate (KH_2PO_4, ACS 99%) were also obtained from Alfa Aesar (Thermo Fisher company). Sodium Chloride (NaCl), potassium chloride (KCl), sodium hydrogen phosphate (Na_2HPO_4) and potassium dihydrogen phosphate (KH_2PO_4) were used for the preparation of phosphate buffer saline (PBS, pH 7.4) and Deionized (DI) water (Model: MilliQ, Millipore Elix water system, resistivity 18 MΩ cm) was used for the experiment.

S2. Dynamic Light Scattering (DLS) Studies

Scattering studies were carried out using a dynamic light scattering (Delsa Nano C, Beckman Coulter) particle analyzer. The hydrodynamic radius (R_h) was evaluated at various salt amounts with the sequential addition of salt. 2ml of the solution was collected, analyzed and poured back into the beaker. 2ml of the sample was collected again and analyzed. This was done a

total of 7 times to ensure repeatability and take the distribution of R_h into account. The laser wavelength was 658 nm, and the scattering angle was fixed at 165°. The data processing was done using the CONTIN algorithm. Stokes-Einstein equation (equation 1) was used to calculate the R_h.

$$D = \frac{k_B T}{6\pi\eta R_h} \quad (1)$$

Where, D = Translational Diffusion Coefficient, k_B = Boltzmann Constant, T = Temperature, η = Viscosity of the solution, R_h = Hydrodynamic Radius.

The temperature of the system was maintained at 40 ºC. The aqueous gelatin solution was analyzed at pH 3.75 and pH 7.5 in dilute and semi-dilute concentration regimes. The two pH were chosen keeping in mind the fact that hydrolysis of gelatin takes place at a pH<3 and pH>10 leading to the breakage of the peptide bonds (**Figure S1**). The concentration for the dilute (1%) and semi-dilute (5%) regimes have been fixed based on the overlap concentrations of gelatin obtained at pH 3.75 (2.5%) and pH 7.5 (3.5%) (**Figure S2a**). Once the dilute and semi-dilute regime was finalized, the DLS analysis was carried out for each salt amount (pure gelatin, 0.4%, 0.8%, 1.6%, 3.2%, 4.8% w/v NaCl with a gap of 15 mins in between) with 7 times repetition. A sequential analysis protocol is followed (shown in **figure S2b**).

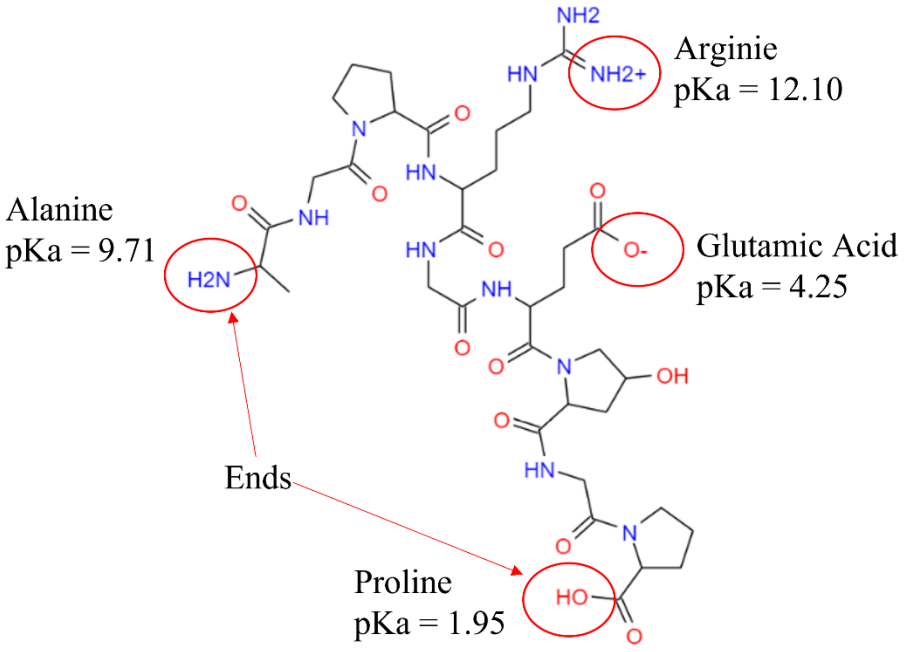

Figure S1. Gelatin monomer structure used for simulation. According to this, a pH > 4.25 will yield a total zero charge on the molecule and 1.95< pH< 4.25 will yield a '+n' charge on the molecule where 'n' is the number of monomers. As lower pH can't be used due to the hydrolysis of peptide bonds, a pH of 3.75 was chosen.

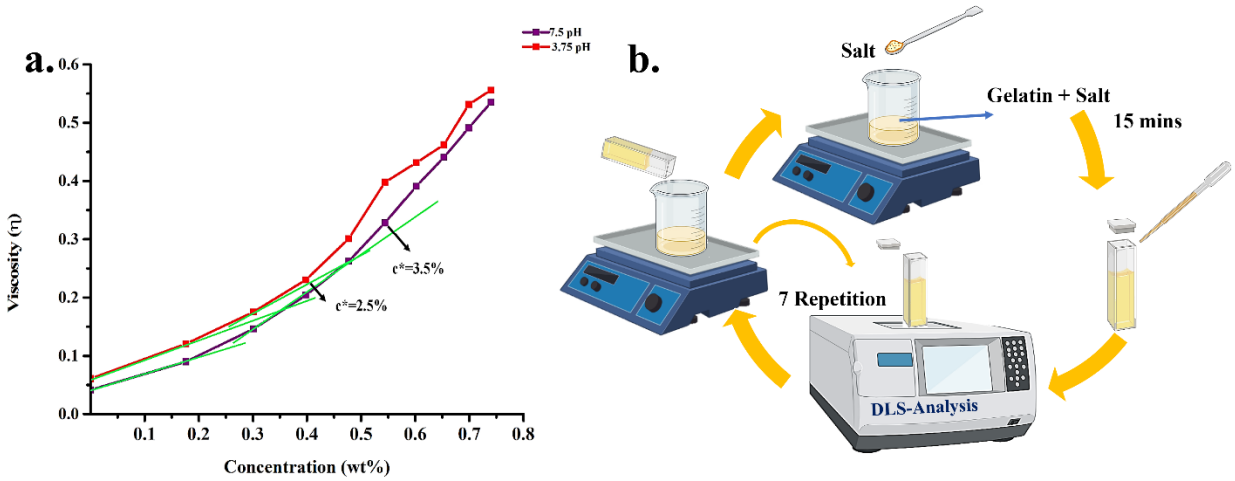

Figure S2. a) Specific viscosity of gelatin with increasing gelatin concentration at 40°C at pH 3.75 and 7.5. The overlap concentration of gelatin is found to be 2.5%. at pH 3.75 and 3.5% at pH 7.5. b) Sequential analysis protocol followed for DLS studies.

Violin plot and Kernel density distribution

The violin plots visualize the distribution of data using probability density estimation. It is an amalgamation of box plots and the kernel density estimate. The violin plots are plotted using MATLAB R2022a. In the case of the violin plot the individual density, curves are built around the center lines unlike that kernel density where they are on the baseline as indicated in **figure S3**. Wider areas of the violin plots represent a higher probability of observations whereas smaller areas indicate a lower probability. The two ends of the violin represents the maximum and minimum values of the data. It is used preferably when the data obeys multimodal non-Gaussian statistics.

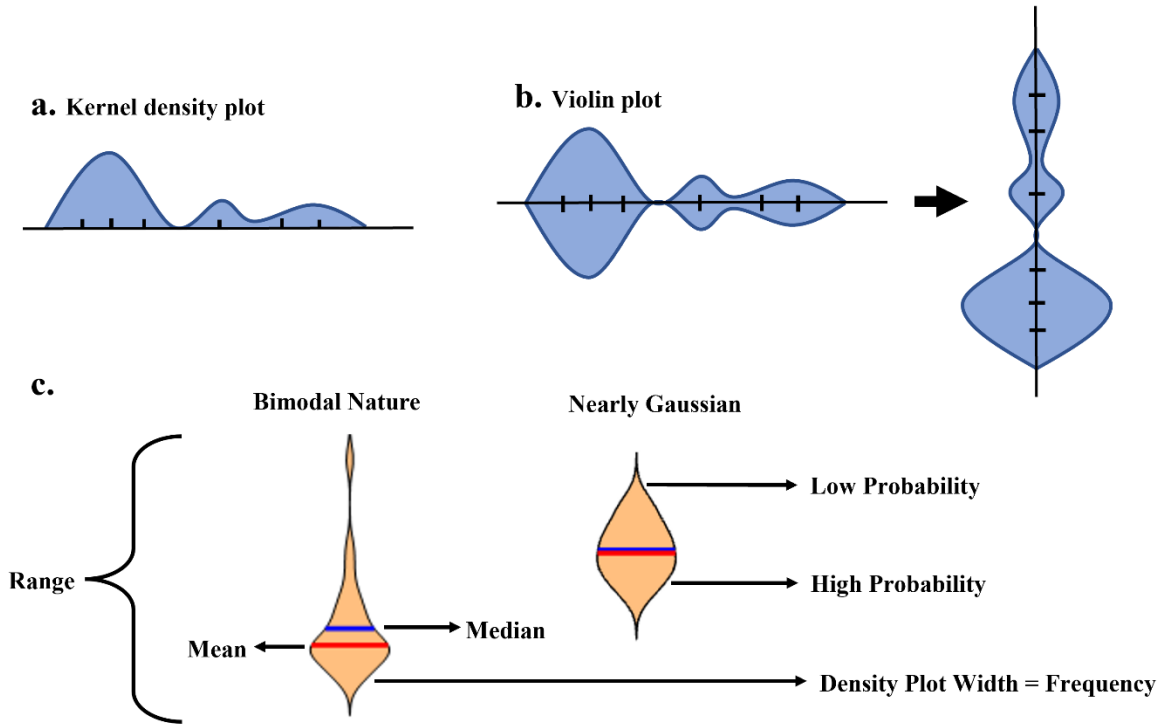

Figure S3. Violin Plot and kernel density estimation

To compare the size distribution of the chains obtained in different cases, a kernel density function was fitted to the data at various salt amounts using MATLAB R2022a and a probability density estimation was constructed.

Quantile-Quantile Plot (Q-Q Plot)

Q-Q plot is a probability plot used to compare two probability distributions. The quantiles of the data are plotted against the theoretical quantiles of a nonmal distribution. The line in the **figure S4** represents the normal distribution and the plus symbols indicate the R_h of the gelatin chains. The spread of the plus symbols from the linear line represents the deviation of the data from normality using the linear fit R^2 value.

Coefficient of Variance (CV)

The Coefficient of variance was calculated as a measure of fluctuation as shown in **table S1**. below. It was calculated as the ratio of standard deviation σ, to mean μ (equation 2). The C_V value if found to be increasing with increasing salt content. A value of C_V greater than 0.35 indicates a scale-up in the fluctuations.

$$CV = \frac{standard\ deviation\ (\sigma)}{mean\ (\mu)}$$

(2)

Table S1. Coefficient of variation (CV) values for pH 7.5 and 3.75

NaCl (%w/v)	CV pH 7.5	CV pH 3.75
0	0.1034	0.1576
0.4	0.1039	0.2095
0.8	0.1173	0.3840
1.6	0.1367	0.3377
3.2	0.3521	0.2855
4.8	0.3201	0.5701

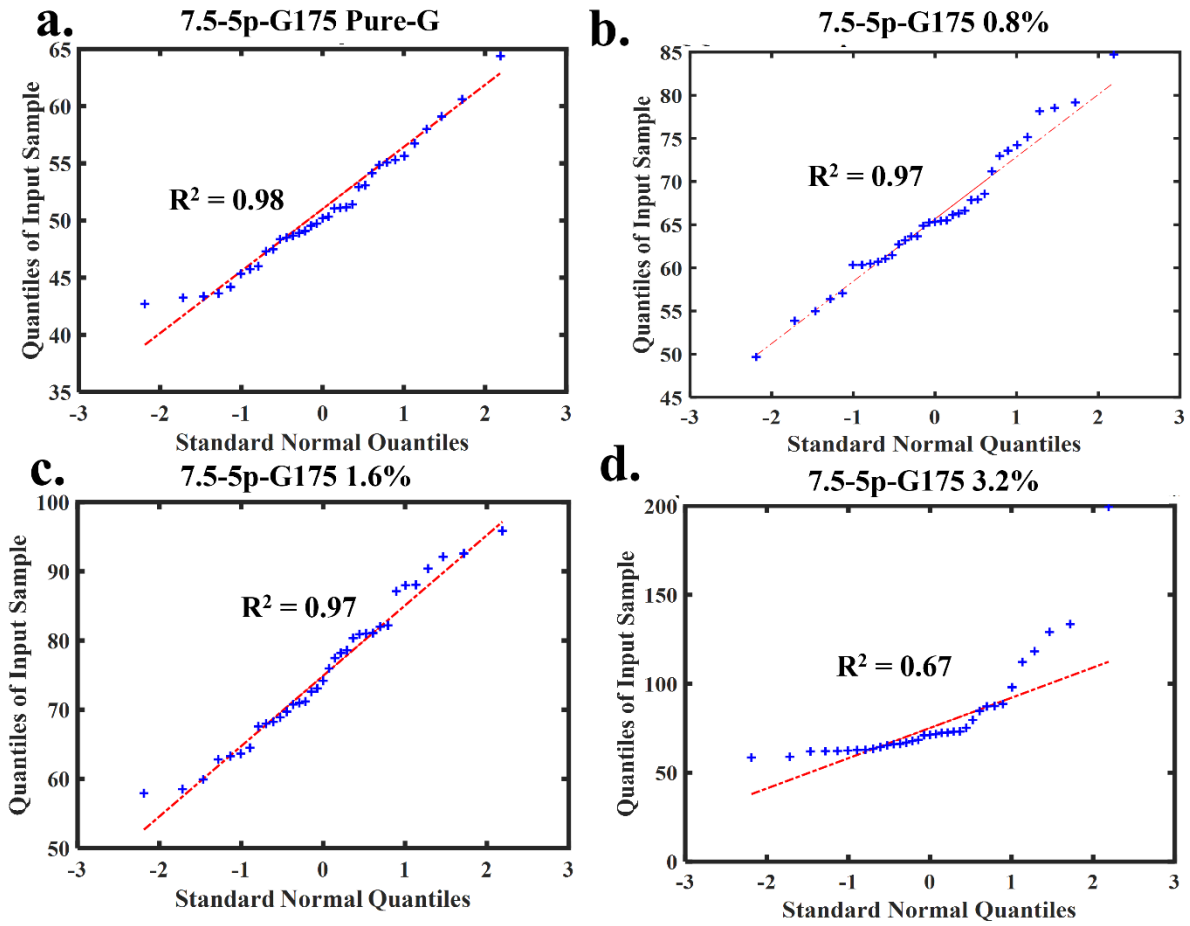

Figure S4. Quantile-quantile plot of R_h data (blue plus sign) and theoretical quantiles (red dotted line) for pH7.5-5p-G175. The linear fit of the R_h data to the theoretical quantile is given by R^2 value. $R^2 = 0.99$ indicates a normal distribution, with more salt the value deviates from 0.99.

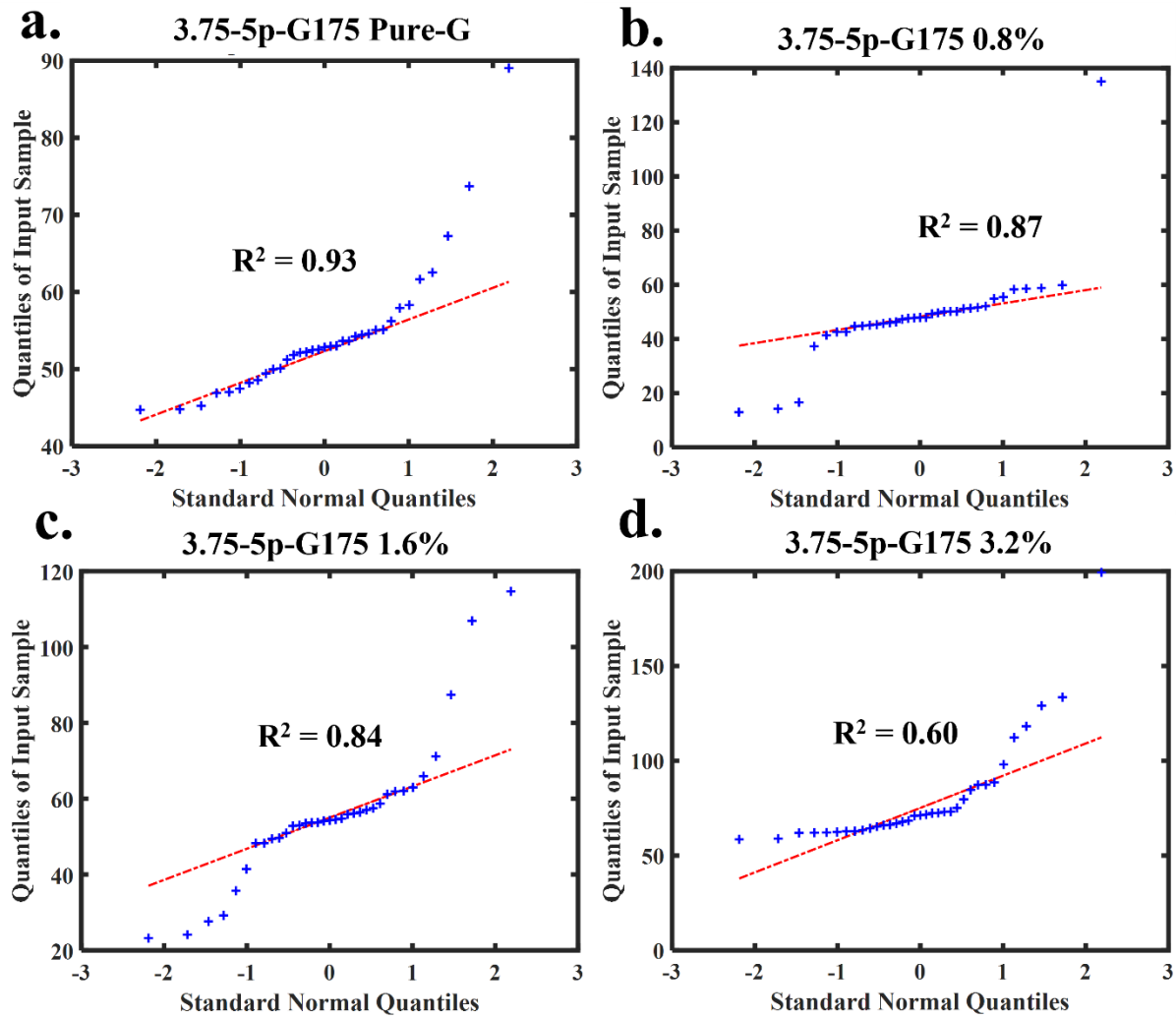

Figure S5. Quantile-quantile plot of R_h data (blue plus sign) and theoretical quantiles (red dotted line) for pH3.75-5p-G175.

S3. Molecular Dynamics Simulation

GROMACS (GROningen Machine for Chemical Simulation, version 2019.5) was used for performing all the MD (molecular dynamics) simulations.[1] OPLSAA forcefield was used to treat all the polymer atoms[2] with periodic boundary conditions in all three dimensions. The SPC/E water model was adopted for the water molecules.[3] These parameters give much more realistic results when compared with the experiment (for liquid water). SMILES (Simplified Molecular Input Line Entry System) text was used as an input to Avogadro (version 1.2.0) software[4] to construct the molecular structure. The molecular geometry obtained from the

Avogadro software was used as the initial configuration of gelatin. The GROMACS topology was generated through TopolGen (version 1.1). This script provides an initial topology file that requires modifications. The atoms section of the topology was modified with respect to the atom types of the corresponding amino acid residues and the partial charges are denoted for all atoms as per the OPLS-AA forcefield parameters defined charges. The files required modifications and were done by building script files for the polymer. VMD (Visual Molecular Dynamics, version 1.9.3) software was used as a visualization tool.[5] The energy minimization was conducted for each system to avoid any steric repulsions using the steepest descent algorithm until a maximum force of lesser than 1000 KJ/mol/nm was reached. A 5 ns NVT simulation was performed with the energy-minimized structure, followed by a 10 ns MD production with a time step of 1 fs. The leapfrog algorithm was employed to integrate the equation of motion. LINCS algorithm was used to constrain the bonds involving H atoms.[6] Nosé-Hover thermostat was used for temperature coupling at 313 K.[7] The particle mesh Ewald (PME) method was utilized to compute long-range electrostatic interactions.[8] The cut-off distance for van der Waals and the short-range electrostatic interactions were taken as 1 nm. To calculate the number of hydrogen bonds, the distance between the donor and acceptor should be less than 0.35 nm and the angle between the hydrogen atom, donor atom and acceptor atom should be less than 30 degrees. Upon completion of the NVT equilibration, a 10ns production was conducted with a time step of 1fs and checked for the stabilization of the structural properties (R_g) and RDF evolution to stabilize. If the structural properties have not stabilized, the simulation is extended for another 10 ns with a reduced time step (0.5 fs). The evolution of radius of gyration (R_g) and the radial distribution function (RDF) of the system for every nanosecond was used as a criterion to check system equilibration. The **figure S6** shows the stabilization of R_g. The simulation trajectory of the MD production run for the last 1000 snapshots separated by 5 ps was used to calculate the average and standard deviation over

all the statistics. Five gelatin chains of molecular weight 8000 g/mol were used for 175 bloom. While calculating box length it was also ensured that the chain length is always less than half of the simulation box ($r < L/2$). The experimental 5% w/v concentration was used to equivalently calculate the final cubic box length (11.5 nm). To consider the starvation effect, at first pure gelatin was run to check the stabilization of RDF with increased amount of water. Once the number of molecules of water was obtained, that final equilibrated state was utilized to add salt sequentially as per the experimental protocol. Each Na^+ can capture 4 molecules of water and each Cl^- can capture 1 molecule of water. The exact amount of required water was added only for the 80mg salt to mimic the experimental condition of no starvation at this salt amount. The isoelectric point of gelatin type-A is 8. In the simulation, the isoelectric point is taken as pH 7 as the number of positive and negative charges are equal and the net charge on the polymer is zero at pH 7 which is equivalent to the experimental pH of 7.5. For pH 3.75, pre-ionized gelatin chains were used to mimic the experimental conditions. The experimental molecular weight of 175 bloom gelatin is 88,087 Da as obtained from Gel Permeation Chromatography (GPC, **Section S6**). In simulation, accounting for a high molecular weight chain results in a huge amount of computational time hence, 8000 Da ($1/10^{th}$) was chosen for 175-bloom gelatin in simulation. This value has also shown comparable results with experimental data and thus was fixed as a standard for 175 bloom.[9] The experimental molecular weight of 300-bloom gelatin is 1,85,000 Da (GPC, **Section S6**). To maintain the same proportionality 21 monomers (1,85000/88087 ~ 21/10) were used for 300-bloom.

OPLS-AA forcefield parameters

The OPLS-AA forcefield parameters are the force constants k, the r_o and θ_o are the equilibrium bond and angle, the Fourier coefficients V, the partial charges on each atom q, and the Lennard−Jones radii and well depths, σ and ε. The geometric combining rules used for the Lennard−Jones coefficients are: $\sigma_{ij} = (\sigma_{ii}\sigma_{jj})^{1/2}$ and $\varepsilon_{ij} = (\varepsilon_{ii}\varepsilon_{jj})^{1/2}$.[10] To retain compatibility, all

the parameters were used without any modifications as developed by Jorgensen and co-workers.[2]

$$E_{bonds} = \sum_i k_{b,i}(r_i - r_{o,i})^2 \quad (1)$$

$$E_{angles} = \sum_i k_{b,i}(\theta_i - \theta_{o,i})^2 \quad (2)$$

$$E_{torsion} = \sum_i \left[\begin{array}{l} \frac{1}{2}V_{1,i}(1 + \cos\varphi_i) + \frac{1}{2}V_{2,i}(1 + \cos 2\varphi_i) \\ + \frac{1}{2}V_{3,i}(1 + \cos 3\varphi_i) + \frac{1}{2}V_{4,i}(1 + \cos 4\varphi_i) \end{array} \right] \quad (3)$$

$$E_{nonbond} = \sum_i \sum_{j>i} \left\{ \frac{q_i q_j e^2}{r_{ij}} + 4\varepsilon_{ij}\left[\left(\frac{\sigma_{ij}}{r_{ij}}\right)^{12} - \left(\frac{\sigma_{ij}}{r_{ij}}\right)^{6} \right] \right\} \quad (4)$$

All the other parameters like, partial charges on each atoms, sigma, epsilon, angle, dihedral and improper coefficients were taken from the original OPLS-AA forcefield parameter files present in the gromacs directory. The amino acid sequence of gelatin monomer used is as follows:

—Proline-Glycine-Hydroxyproline-Glutamic Acid-Glycine-Arginine-Proline-Glycine-Alanine—

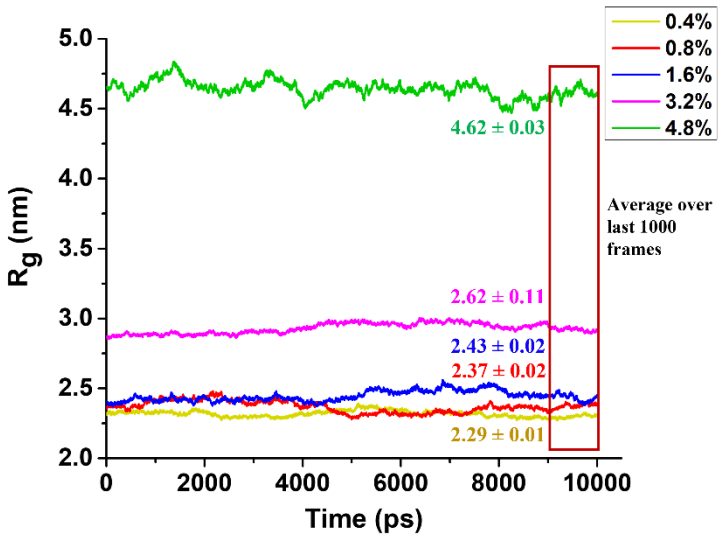

Figure S6. Evolution of R_g over time obtained from simulation for different NaCl concentration (% w/v).

S4. Preparation of sodium alginate - gelatin hydrogel and in-vitro drug release study

5% (w/v) Gelatin was dissolved in 20 mL of solvent (pH 7.5 and pH 3.75) at 40 °C. Once the gelatin is totally dissolved the required amount of NaCl is added. After 15 mins of intervals 30 mg naproxen sodium was added. After 15 mins, 4g of sodium alginate was added and stirred. The hydrogel is completely dried at 37 °C before the experiment. The drug-loaded hydrogel was immersed in 100 mL PBS (pH-7.4) at 37 °C and stirred at 100 rpm to mimic the intestine condition, where the drug absorption takes place. 3 mL of aliquots were collected, and an equivalent amount of PBS was added to maintain the total volume. UV-VIS spectroscopy (Lab India Analytical UV 3092) was performed to analyze the drug concentration (at 272nm λ_{max}).

S5. FTIR/ATR Analysis

The FTIR analysis was carried out using Bruker Tensor 37, Miracle Single Reflection Horizontal ATR accessory. The spectral range was collected between 600cm^{-1} to 4000 cm^{-1} with a spectral resolution of 4 cm^{-1} and 256 scans were performed. The spectra between 1600-1700 cm^{-1} (Amide-I band) were deconvoluted to obtain the variation in the secondary structures of the protein. The hidden peaks were obtained by considering the second derivative of the amide-I band using the Savitsky-Golay algorithm with a 7-point smoothening window in OriginPro9.[11] The experimental method was similar to that in DLS. The fluctuations were mapped by analyzing the sample 5 times at a 5-minute intervals.

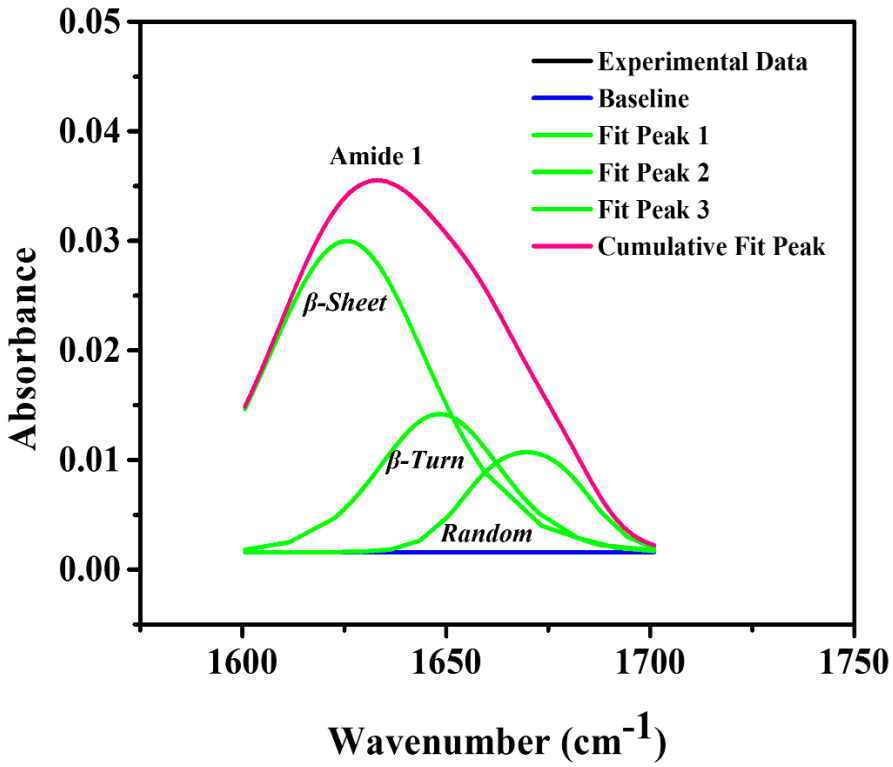

Figure S7. Deconvoluted peaks from FTIR/ATR depicting the different protein secondary structures.

Section S6. Gel Permeation Chromatography (GPC)

The molecular weight of gelatin type-A 175 bloom and 300 bloom was determined using Malvern OmniSec gel permeation chromatography (GPC) fitted with an aqueous column of Viscotek A4000 having a molecular weight cut off 10L Da. An isocratic pump fitted with a degasser was used in the setup. Phosphate buffer saline (PBS) of pH 7.4 was used as the mobile phase with a flow rate of 0.8 mL/min. 0.2 mg/mL of gelatin was dissolved in the mobile phase and filtered through 0.22-micron cellulose-acetate filters for analysis. The sample injection volume was 50 µL. The temperature of the column oven, and detector oven was fixed at 30 °C. The autosampler temperature was at 25 °C. The molecular weight was estimated using calibrated pullulan 118 kDa standard.

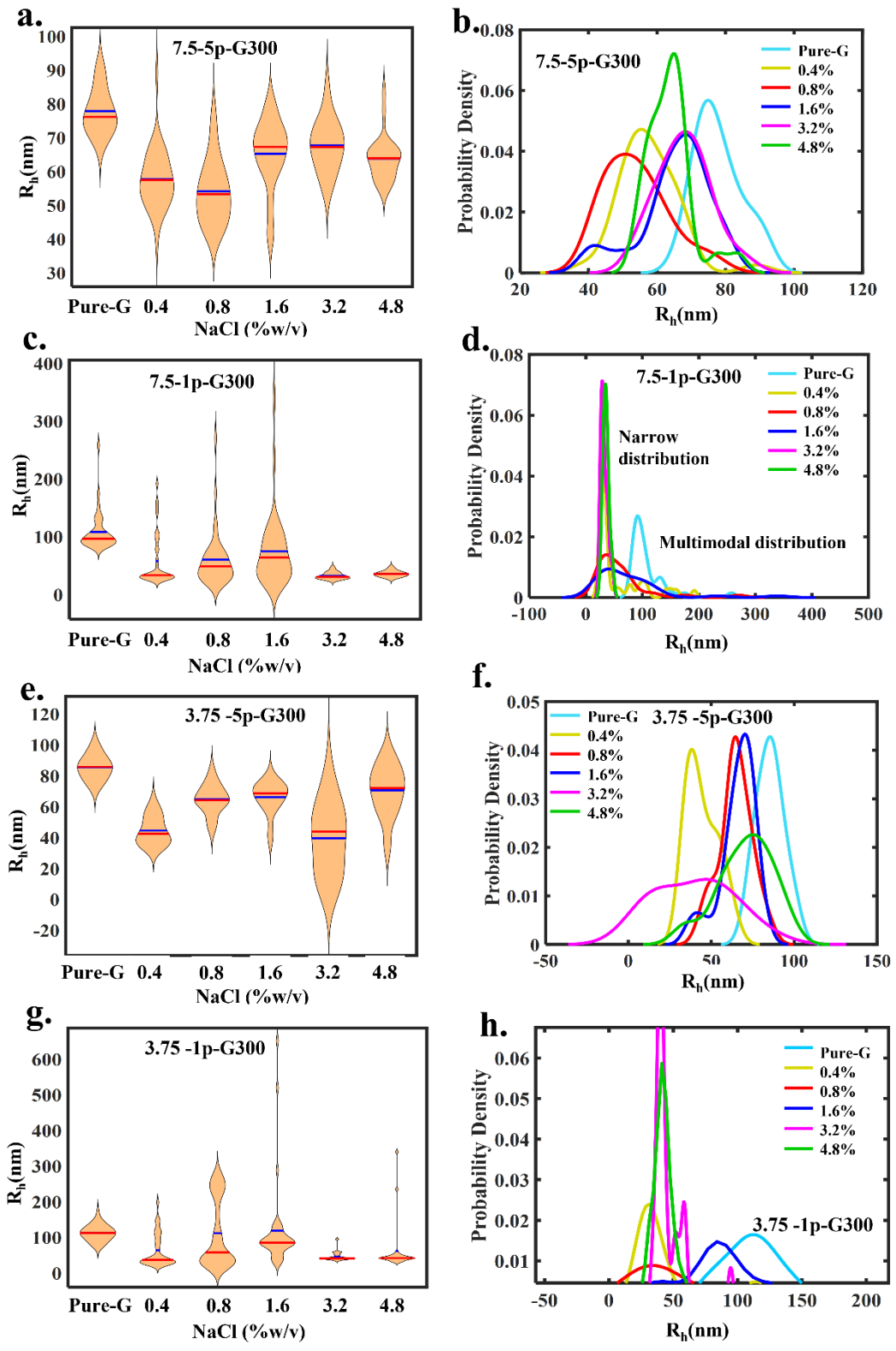

Figure S8. Violin Plot for R_h with the increasing NaCl %(w/v) (Red-mean, Blue-median). Non-parametric Kernal density fitted to obtain the distribution of R_h of gelatin chains at various NaCl %(w/v) at semidiute and dilute regime for pH 7.5 -G300 and pH 3.75 -G300.

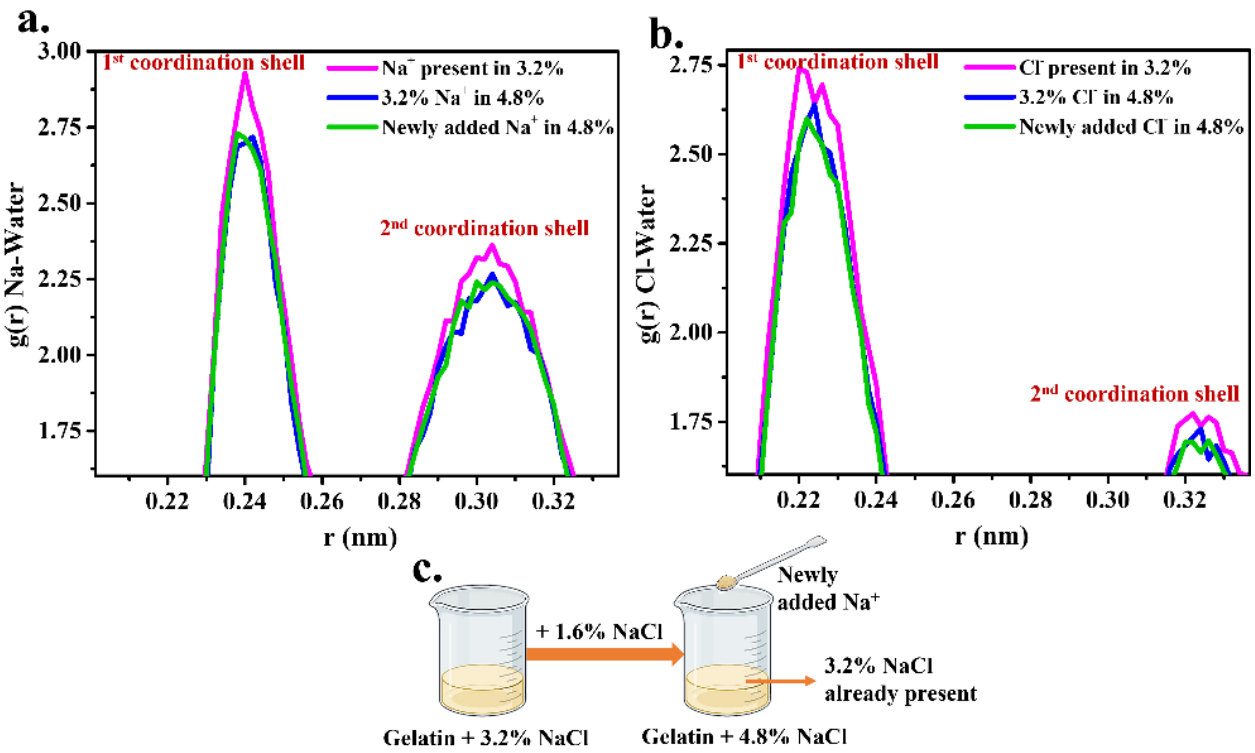

Figure S9. Radial Distribution Function (RDF) for Na-water and Cl-water for 3.2% and 4.8% NaCl. The legend **Na^+ present in 3.2%** shows the RDF for Na-water only for extra Na^+ ions present in the 3.2% NaCl case. **3.2% Na^+ in 4.8%** represents the Na^+ ions of 3.2% NaCl present in 4.8% NaCl. **Newly added Na^+ in 4.8%** represents the extra Na^+ ions of 4.8%.

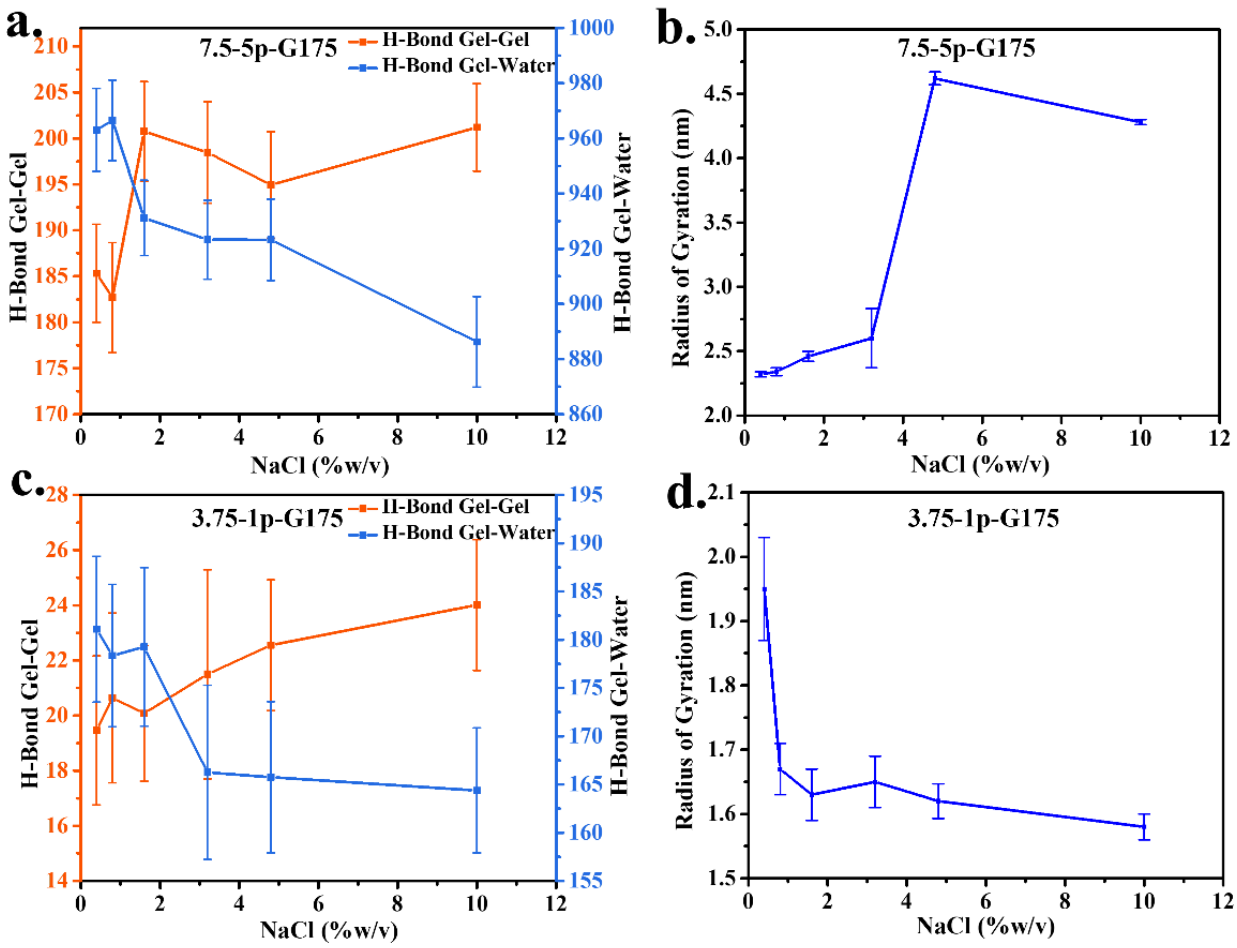

Figure S10. pH 7.5 -5p -G175. a) H-Bonds between gelatin-gelatin and gelatin-water; b) Radius of gyration of gelatin. pH 3.75 -1p -G175. c) H-Bonds between gelatin-gelatin and gelatin-water; d) Radius of gyration of gelatin. In the case of 5%w/v gelatin, 5 chains were used in the simulation whereas for dilute cases only 1 chain has been used. Due to this, the availability of donors and acceptors is lower in the dilute case compared to the semidilute case. Thus, the variation for hydrogen bonds in dilute cases is higher than that of semidilute cases. Moreover, for pH 3.75 the hydrogen bonds count (14-28) is lesser than pH 7.5 (170-280) as gelatin chains are elongated at pH 3.75 due to the electrostatic repulsion among the NH_3^+ groups. Whereas at pH 7.5, the donor and acceptor are sufficiently close as it is in a collapsed state at the isoelectric point, hence a larger number of hydrogen bonds.

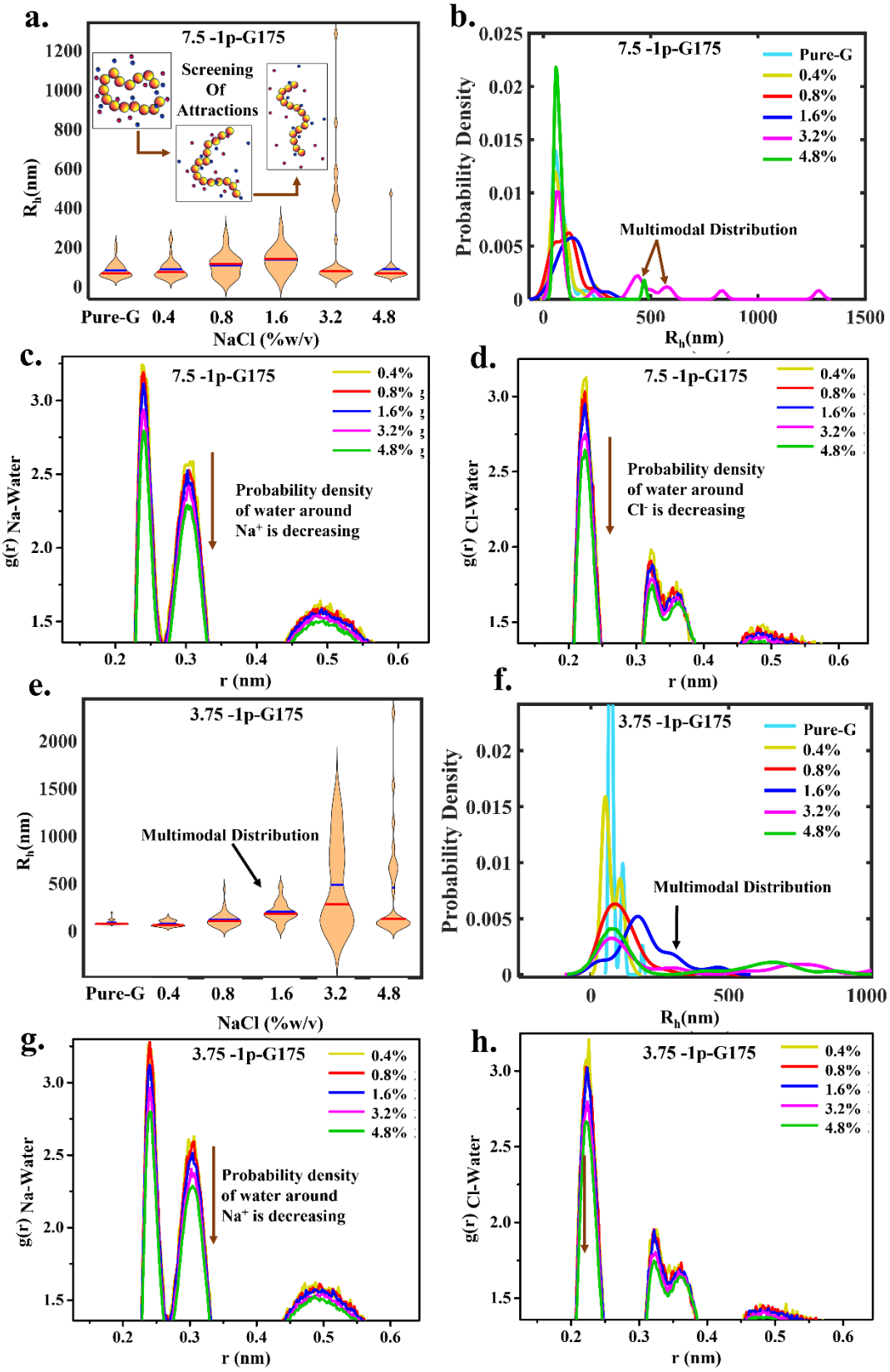

Figure S11. Violin plot with mean (red line), median (blue line) of R_h with the addition of salt, a) pH 7.5 -1% -G175. Kernel density function fitted to the R_h distribution, b) pH 7.5 -1% -

G175. Radial distribution function (RDF) for: c) Na-water; d) Cl-water. Violin plot with mean (red line), median (blue line) of R_h with the addition of salt, e) pH 3.75-1% -G175. Kernel density function fitted to the R_h distribution, f) pH 3.75-1% -G175. Radial distribution function (RDF) for: g) Na-water; h) Cl-water.

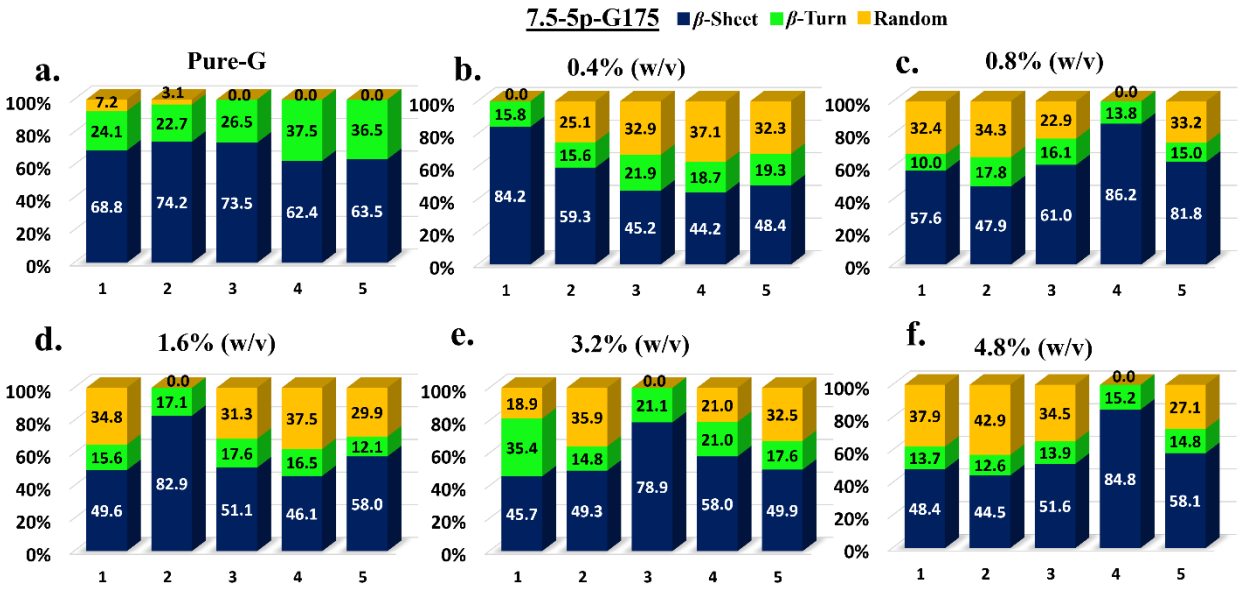

Figure S12. Fluctuations in protein secondary structure for pH 7.5 -5p -G175.

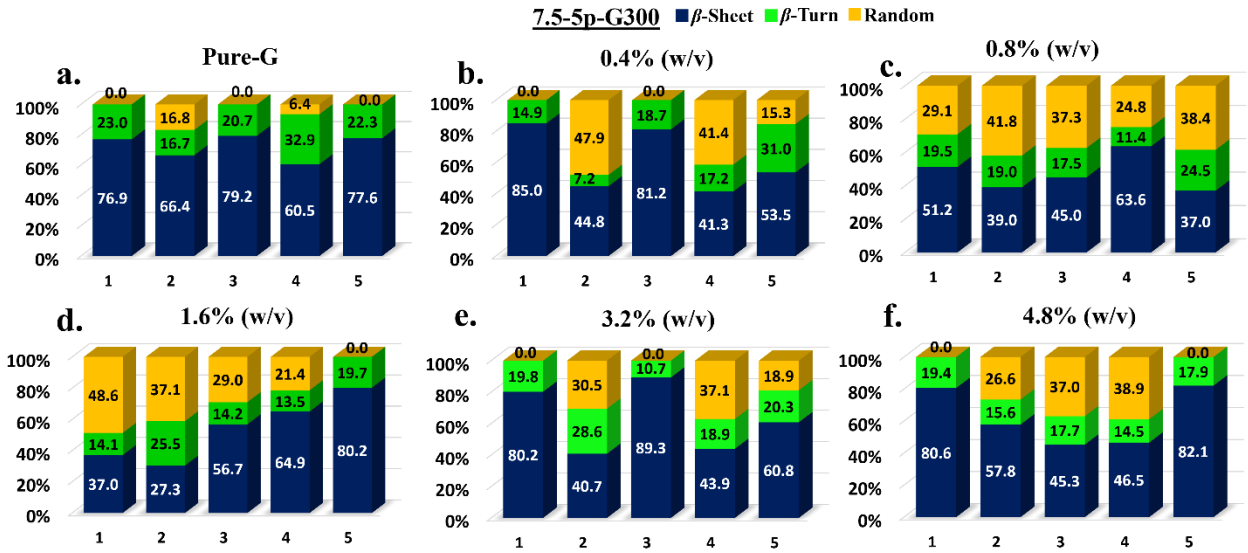

Figure S13. Fluctuations in protein secondary structure for pH 7.5 -5p -G300.

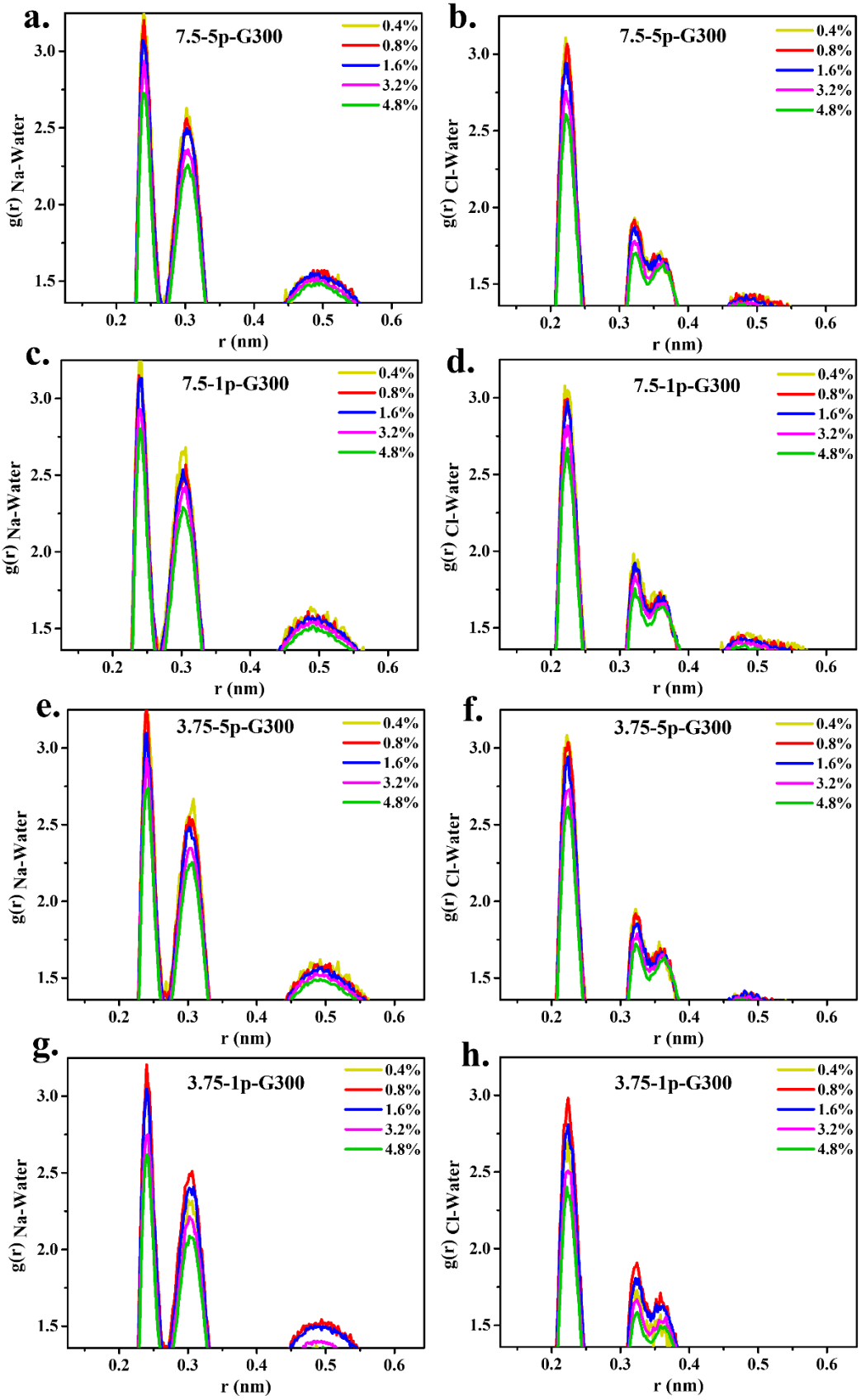

Figure S14. Radial Distribution Function (RDF) for pH 7.5 -5p -G300. a) Na-water; b) Cl-water; Radial Distribution Function (RDF) for pH 7.5 -1p -G300. c) Na-water; d) Cl-water.

Radial Distribution Function (RDF) for pH 3.75 -5p -G300. e) Na-water; f) Cl-water; Radial Distribution Function (RDF) for pH 3.75 -1p -G300. g) Na-water; h) Cl-water.

References

1 M. J. Abraham, T. Murtola, R. Schulz, S. Páll, J. C. Smith, B. Hess and E. Lindahl, *SoftwareX*, 2015, **1**–**2**, 19–25.

2 W. L. Jorgensen and J. Tirado-Rives, *J. Am. Chem. Soc.*, 1988, **110**, 1657–1666.

3 P. Mark and L. Nilsson, *J. Phys. Chem. A*, 2001, **105**, 9954–9960.

4 M. D. Hanwell, D. E. Curtis, D. C. Lonie, T. Vandermeersch, E. Zurek and G. R. Hutchison, *J. Cheminform.*, 2012, **4**, 17.

5 W. Humphrey, A. Dalke and K. Schulten, *J. Mol. Graph.*, 1996, **14**, 33–38.

6 B. Hess, H. Bekker, H. J. C. Berendsen and J. G. E. M. Fraaije, *J. Comput. Chem.*, 1997, **18**, 1463–1472.

7 W. G. Hoover, *Phys. Rev. A*, 1985, **31**, 1695–1697.

8 T. Darden, D. York and L. Pedersen, *J. Chem. Phys.*, 1993, **98**, 10089–10092.

9 T. Basu, U. Bhutani and S. Majumdar, *J. Mater. Chem. B*, 2022, **10**, 3614–3623.

10 B. Doherty, X. Zhong, S. Gathiaka, B. Li and O. Acevedo, *J. Chem. Theory Comput.*, 2017, **13**, 6131–6145.

11 H. Yang, S. Yang, J. Kong, A. Dong and S. Yu, *Nat. Protoc.*, 2015, **10**, 382–396.